Med Biol Eng Comput (2010) 48:945–954
DOI 10.1007/s11517-010-0644-8

SPECIAL ISSUE - REVIEW

Flexible and stretchable micro-electrodes for in vitro and in vivo neural interfaces

Stéphanie P. Lacour · Samia Benmerah · Edward Tarte · James FitzGerald · Jordi Serra · Stephen McMahon · James Fawcett · Oliver Graudejus · Zhe Yu · Barclay Morrison III

Received: 12 January 2010 / Accepted: 27 May 2010 / Published online: 10 June 2010

Abstract Microelectrode arrays (MEAs) are designed to monitor and/or stimulate extracellularly neuronal activity. However, the biomechanical and structural mismatch between current MEAs and neural tissues remains a challenge for neural interfaces. This article describes a material strategy to prepare neural electrodes with improved mechanical compliance that relies on thin metal film electrodes embedded in polymeric substrates. The electrode impedance of micro-electrodes on polymer is comparable to that of MEA on glass substrates. Furthermore, MEAs on plastic can be flexed and rolled offering improved structural interface with brain and nerves in vivo. MEAs on elastomer can be stretched reversibly and provide in vitro unique platforms to simultaneously investigate the electrophysiological of neural cells and tissues to mechanical stimulation. Adding mechanical compliance to MEAs is a promising vehicle for robust and reliable neural interfaces.

Keywords Micro-electrodes · Polymers · Compliance · Action potentials · Field potentials · Peripheral nerve · Slice culture

S. P. Lacour (✉)
Department of Engineering, Nanoscience Centre, University of Cambridge, 11 JJ Thomson Avenue, Cambridge CB30FF, UK
e-mail: spl37@cam.ac.uk

S. Benmerah · E. Tarte
Department of Electrical Engineering, University of Birmingham, Birmingham BT152TT, UK

O. Graudejus
Centre for Adaptive Neural Systems, Arizona State University, Tempe, AZ 85287, USA

Z. Yu · B. Morrison III
Department of Biomedical Engineering, Columbia University, New York, NY 10027, USA

J. FitzGerald · J. Fawcett
Centre for Brain Repair, University of Cambridge, Cambridge CB20PY, UK

J. Serra · S. McMahon
London Pain Consortium, King's College London, London SE11UL, UK

1 Introduction

Electrode arrays designed for recording and stimulation of neural activity are widely used in neurological research as well as clinical therapy. Most of these arrays are microfabricated using MEMS technology and stiff materials including silicon, glass and metals. Dense arrays of up to 256 electrodes are used in vitro to monitor/stimulate individual neurons or acute tissue slices [14, 27] and in vivo to treat or repair damaged brain tissues or peripheral nerves [16, 31]. These 2D arrays interface very well with neurons' population cultured in vitro or 2D-organized neural networks in vivo such as ganglionic neurons in the retina. However, rigid microelectrode arrays (MEAs) do not provide long-term and robust interfaces when interfaced with 3D neural tissues such as a nerve, or when mechanical stimulation is applied to the probed tissue.

In this article, we describe the technology and design of mechanically compliant neural MEAs, and current prototypes for in vitro and in vivo applications. The focus of these soft neural interfaces is on extracellular recording of action or field potentials but extracellular stimulation can also be implemented.

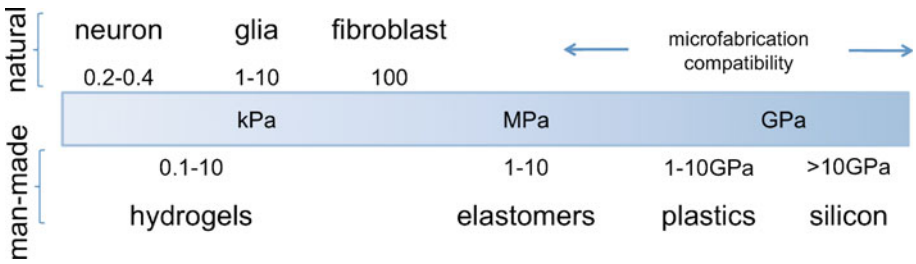

Fig. 1 Mechanical scale illustrating the elastic modulus of man-made and natural materials

The mechanical mismatch between man-made device materials for MEAs and biological tissues and cells is clearly illustrated Fig. 1. Cells are soft and visco-elastic with well-defined mechanical properties characterized by elastic modulus in the range of 100s to 1,000s Pa. In vivo, they are surrounded by other cells and extracellular matrix. In vitro or when interfaced in vivo with man-made implants, cells are in contact with materials that are many orders of magnitude stiffer. For example, silicon and glass are brittle materials with Young's modulus of hundreds of GPa. An increasing number of studies focused on cells' biomechanics highlight that cells can be extremely sensitive to changes in the mechanical properties of their surroundings, occurring independently of the biochemical environment [4, 18, 29, 35]. In vivo, implanted electrodes trigger a foreign body reaction leading to chronic inflammation and scar formation [34]. Fibrotic tissue encapsulates the recording and stimulating sites of the electrodes, and prevents reliable and long-term electrophysiology.

Furthermore, in vivo biological tissues withstand moderate and repeated mechanical deformations to accommodate movements around joints. During traumatic injuries, neural tissues may experience violent mechanical stretch with strains of tens of percent.

The design of electrode arrays falls into one of following categories: planar, penetrating, cuff, and regenerating electrodes.

Planar electrodes are metallic patterns on glass, silicon and more recently polyimide substrates designed for extracellular stimulation and recordings in vitro on various types of tissues or cells, e.g., acute hippocampal slices, primary neurons or organotypic preparations [7]. Electrodes are typically patterned in 8×8 or 6×10 grids over a few mm^2 surface area, but 16×16 arrays are also available [30]. Whilst planar MEAs provide spatial as well as temporal information about neural networks, they are rigid MEAs and thus, cannot monitor neuronal activity from tissues or cells subject to mechanical deformation or injury.

Penetrating MEAs are based on needle-like structures, which are pushed into the brain or the nerve in vivo [15, 19]. They are fabricated with silicon or titanium. They may comprise a single needle bearing multiple contacts on its shaft [20, 39] or a 10×10 matrix of single contact electrodes [19, 36]. Successful penetrating electrodes are already available to humans, e.g., cochlear implants [40] and deep brain stimulator [10, 17]. However, stable and long-term recording and stimulation remain a challenge. One of the recurrent hurdles is the cellular reactive response and increased tissue-electrode impedance due to insertion trauma, tethering and micro-motion of the stiff needle-like electrodes.

Cuff electrodes are insulating polymeric sleeves, which wrap around a nerve and carry electrical contacts on their inner surface [5, 41]. Because they do not penetrate or cut the nerve, cuff electrodes only interface with outer axons; distinguishing between signals from different axons in the same fascicle is then nearly impossible.

Regenerative electrodes are devices inserted to the proximal stump of a sectioned nerve. They provide a structure that allows for nerve fibers outgrowth, and an array of electrodes distributed across the nerve's cross-section, often referred to as sieve electrodes [6, 41]. The sieve is prepared as "transparent" as possible to guarantee robust axon regeneration. However, sieve MEAs usually have a modest number of electrodes (up to 12) given the conflict between hole space and lead-out space [31]. Furthermore, long-term (>12 month post-implantation) reliability of regenerative implants has not been reported.

Therefore, the challenge lies in finding technological routes to produce electrode arrays, which disrupt minimally the cells' environment so that (i) they behave in vitro like in the body, (ii) they induce in vivo minimal inflammatory response, (iii) they provide long-term communication between neural fibers and electronic hardware, and (iv) when needed, they conform and deform along with the 3D neural tissue.

In this article, we propose to use thick polymer microtechnology to design and fabricate improved MEAs. We report on the fabrication and electromechanical characterization of flexible (polyimide-based) and stretchable (silicone-based) MEAs. We further illustrate the potential of compliant micro-electrodes for neuronal electrical interfaces.

2 Methodological consideration

2.1 Microfabrication

Electrode arrays are composed of a substrate, a pattern of metallic tracks defining the electrodes and their interconnections and an electrically insulating encapsulation coating. Soft micro-electrodes are designed using structural polymer materials. The fabrication process of compliant MEAs is illustrated Fig. 2a. Depending on the application, the polymer may be a plastic, e.g., polyimide, or an elastomer, e.g., silicone. The overall process flow is independent of the selected polymer.

Compliant MEAs are processed on a rigid carrier, e.g., a silicon wafer or a glass slide. First, the polymer substrate is spin-coated on the carrier to form a uniform film of tens of microns thickness, and cured according to manufacturers' specifications. Then, the electrode stack is evaporated on the polymer substrate and patterned using conventional photolithography. The patterned electrodes are then encapsulated with a second polymeric film. Electrode sites and contact pads are opened in the encapsulation coating either by etching away the polymer using reactive ion etching or by UV insulating and developing the photopatternable polymer. The polymer/electrode/polymer structure is then cured and peeled-off manually from the rigid carrier.

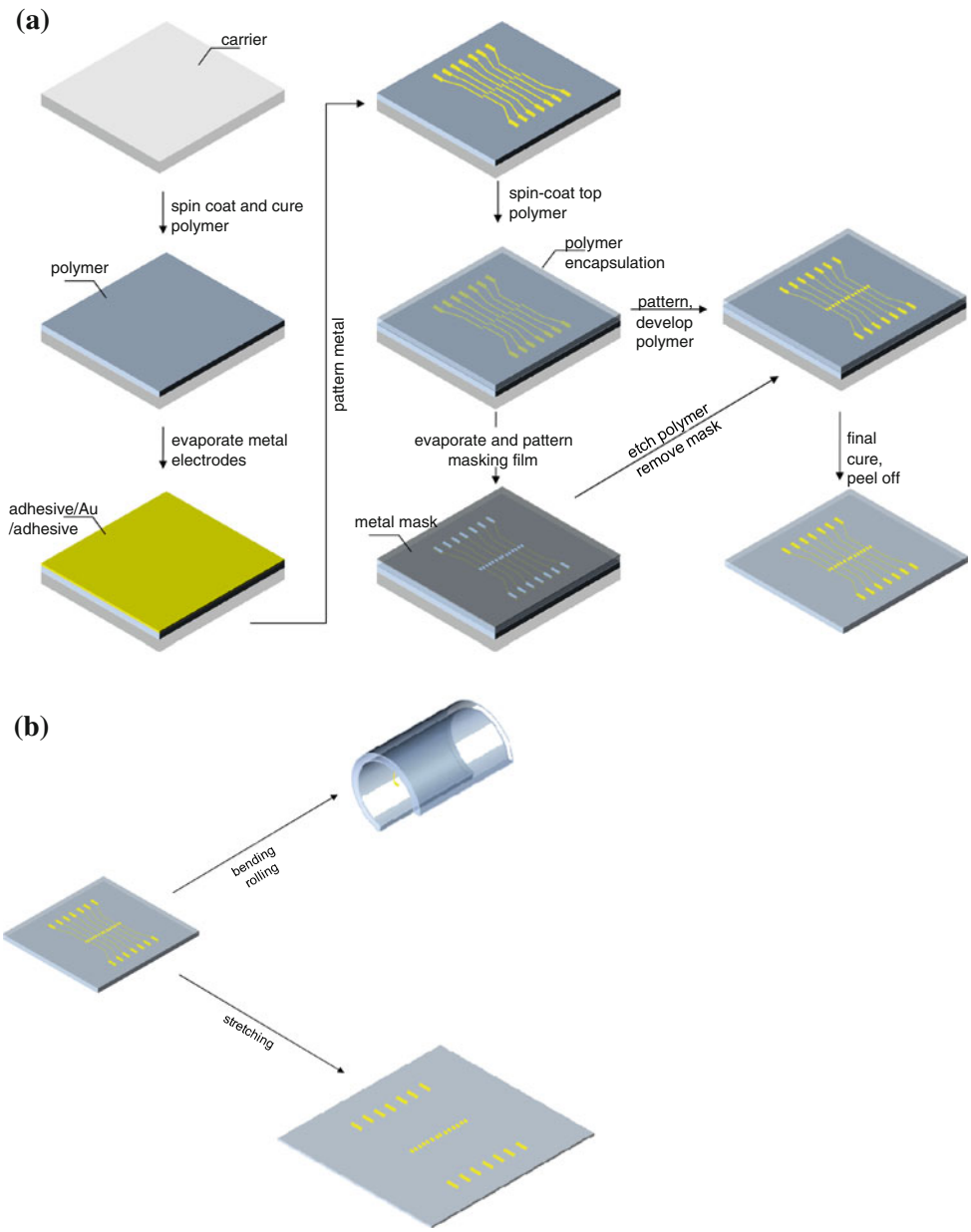

Fig. 2 Micro-fabrication of compliant neural interfaces. **a** Process flow; **b** two deformation modes: bending and stretching

Two compliant MEAs are presented in the following sections: (1) a flexible in vivo regenerative MEA implant based on polyimides, and (2) a stretchable in vitro MEA based on elastomers. Polyimides are Pyralin 2611 HD Microsystems and photosensitive Durimides 7005 & 7020 Fujifilm. Elastomers are Sylgard 184 Dow Corning (polydimethylsiloxane PDMS) and photo-patternable silicone WL5150 Dow Corning. The micro-electrodes are made of a chromium/gold/chromium stack (Cr/au/Cr) with 3–5 nm/50–150 nm/3–5 nm thickness. The recording sites are defined by photolithography; minimum electrodes' dimensions are 30 × 100 μm and 100 × 75 μm when embedded in polyimide and silicone, respectively.

Sterilization of the compliant micro-electrodes is then achieved by autoclave in deionized water at 121°C, 2 atm, for 20 min or by soaking in ethanol for 3 h.

2.2 Mechanical design

Compliant micro-electrodes are designed to be flexed or stretched as shown Fig. 1b.

In bending mode, the MEA is rolled and folded around a central axis. The resulting strain in the electrode film depends on the bending radius (R), the thickness of the polymer/metals/polymer stack, the location of the metal film in the stack and the stack profile. In order to minimize the strain applied to the electrode, the metallic thin film must be positioned at or as close as possible to the neutral plane of the rolled structure (where the strain is null) [37, 38]. In order to do so, the thickness of the substrate (t) and the encapsulation film (e) and the stack profile must be optimized. This strategy is routinely implemented in flexible displays and thin film electronics [3, 37, 38]. The top bending strain ε_{top} in a nonencapsulated metal film (thickness, t_f) on a plastic substrate (thickness, t) is derived as $\varepsilon_{top} = (t - t_f)/2R$ with R the bending radius [37]. Typically, bending strains (which may be tensile or compressive) do not exceed 5% assuming that the stack is thin ($\ll$1 mm) and the smallest radius >150 μm. Thicker stacks with U-shaped profiles can also be designed to guarantee minimal strain in the embedded electrode layer [24].

In stretching mode, the MEA is extended and relaxed in one or several directions simultaneously. Such deformations are encountered in vivo when a nerve extends and relaxes over a joint [13, 26] or during a mechanical injury [28, 42]. Applied tensile strains can reach up to 20% and stretching cycles can occur within milliseconds [28].

Rigid or flexible MEAs cannot sustain such large mechanical deformations, they are either too stiff or fail by mechanical fracture of the metal at small strain. Stretchable metallization was first reported in 2003 [1, 12, 32]: thin gold film conductors on PDMS membrane can stretch and relax by tens of percent strain without electrical failure and over thousands of cyclic loadings. The stretchability of the metal film on PDMS relies on the built-in microstructure of the gold film and on the extreme compliance of the elastomeric substrate [12, 23]. Such stretchable metallization is now implemented to produce ultracompliant MEAs.

2.3 In vitro and in vivo protocols

In vitro experiments were conducted in accordance with Columbia University IACUC, and in vivo experiments were carried out in accordance with the United Kingdom Animals Act, 1986.

2.3.1 Organotypic hippocampal brain slice cultures

Hippocampal slices were prepared as described previously in [42]. In brief, hippocampi from rat pups (9 days old) were removed and sectioned into 40-μm thick slices. The latter were plated directly onto sterile silicone MEAs, which were precoated with laminin and poly-L-lysine. The slices on MEAs were maintained under standard culture conditions (37°C, 5% CO_2) for at least 5 days.

2.3.2 Sciatic nerve implants

Rolled MEA implants were sterilized in 70% ethanol for 3 h and filled with saline before implantation in adult Lewis rats. Surgery was conducted under general anaesthesia using a mixture of intraperitoneal medetomidine (0.25 mg/kg) and ketamine (60 mg/kg), and with sterile precautions. The right sciatic nerve was transected at mid-thigh level, and the stumps stitched into the ends of the polymeric implant. The external connector was positioned subcutaneously. After implantation, muscle and skin were reapproximated and sutured in layers.

2.4 Instrumentation

2.4.1 Electrode characterization

Impedance spectra (modulus and phase) of the electrodes embedded in polyimide and silicone were recorded in saline solution using an HP impedance analyzer in the 100 Hz to 100 kHz frequency range (25–100 mV excitation voltage) [11, 24].

The electrical response of the micro-electrodes was also evaluated as a function of mechanical deformation (bending and stretching). Rolled micro-electrodes in polyimide were tested over a period of 3 months in saline solution; micro-electrodes embedded in PDMS were cycled to strain of up to 20% in customized electro-mechanical stretchers. The stretchers' design is described in detail in [1, 11, 12].

Applied strain and strain rate are in the ranges of 0.1–20%, and 0.2%/s–0.2%/min, respectively.

2.4.2 *Electrophysiology*

2.4.2.1 In vitro recordings Neural activity was recorded from hippocampal slice cultures perfused with artificial cerebrospinal fluid and maintained at 37°C. After 5 days in culture, spontaneous or evoked field potentials from hippocampal slices were recorded using the silicone MEAs interfaced with a MultiChannel system [11, 42]. Evoked signals were triggered with constant current stimulation (0–200 μA in 10-μA steps) using one of the MEA electrodes. After initial recordings, the MEA with adherent slice was biaxially stretched to 8% Lagrangian strain and relaxed. Neural activity was immediately recorded post-injury from the very same electrodes thus providing an accurate mapping of the slice.

2.4.2.2 In vivo extracellular recordings Action potentials from regenerated sciatic nerve fibres were recorded using rolled MEA implants. Recording sessions were performed under terminal general anaesthesia (urethane, 1.25 g/kg, i.p.). At 12 weeks post-implantation, the implant and connector was exposed, and connected to external amplifying, filtering, and recording hardware. Nerve signals resulting from cutaneous stimulation were recorded using individual electrodes in the implant, against a reference electrode inserted into nearby muscle. The recording channel was amplified 1,000×–10,000× and bandpass filtered from 500 Hz to 10 kHz. Signals were then monitored visually and acoustically, and stored with a Tektronix digital storage oscilloscope. Pin electrodes were inserted transcutaneously into the foot and square wave constant current stimuli applied (2-ms duration, 5-mA amplitude). Responses to such stimulation were recorded and averaged, typically for 10–100 sweeps.

3 Practical applications

3.1 Polymeric extracellular electrodes

Figure 3 shows optical micrographs of gold micro-electrodes embedded in polyimide (Fig. 3a) and silicone (Fig. 3b). The polymeric arrays are first manufactured flat; the gold tracks are embedded between upper and lower layers of polyimide or silicone.

Polyimide arrays were prepared with a 25-μm thick Pyralin 2611 substrate (HD Microsystems) and encapsulated with a 5-μm thick photosensitive polyimide layer (Durimide 7505, Fujifilm). The metallic tracks were prepared by thermal evaporation of 150-nm thick gold film on

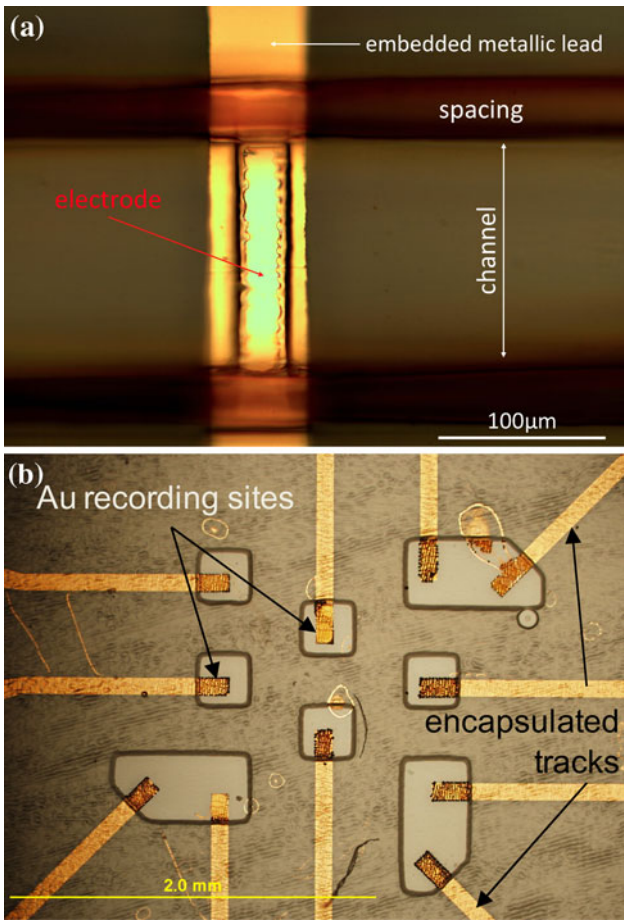

Fig. 3 Optical micrographs of flexible and stretchable micro-electrodes. **a** Top view of a gold electrode sandwiched between a polyimide substrate and a photosensitive polyimide film. The recording site, 30 × 100 μm surface area, is defined by an opening in the top coating. Channel refers to the micro-channel shown Fig. 5 [24]. **b** Top view of a silicone micro-electrode array. Eleven gold electrodes are patterned on a silicone substrate and encapsulated with a photo-patternable silicone. Openings in the top silicone are larger than the electrodes' recording sites [11]

5-nm thick chromium adhesive and patterned by photolithography. Recording sites are typically 30 × 100 μm (Fig. 3a).

Silicone arrays are prepared in a similar sequence using Sylgard 184, Dow Corning, substrate (280 μm thick) and photo-patternable silicone encapsulation (WL5150 Dow Corning, 15 μm thick). Silicones are widely used in the fabrication of hybrid cuff electrodes in combination with platinum foils [33]. Patterning MEA directly onto the elastomeric substrate is of a recent concern [22, 25, 26].

We have optimized the patterning of thin (<100 nm) gold films onto PDMS allowing for the microfabrication of robust and highly stretchable micro-electrodes [1, 11]. Features as small as 30 × 30μm^2 can be defined in 40-nm thick gold film on PDMS with 90% yield, and using standard photolithography [1]. The encapsulation silicone is

typically 10–50 μm thick and allow for the definition of large openings, >50 μm side. Figure 3b illustrates an 11-electrode silicone array with 100 × 200 μm^2 openings in the top silicone defining ~75 × 100 μm electrodes [11].

3.2 Electrode impedance as a function of mechanical deformation

Neural electrodes are used as the electrical point of contact between the action potentials travelling along the neurons and the electronic hardware. The maximum potential change seen extracellularly is a fraction of the action potential's amplitude and is proportional to the ratio $R_{out}/(R_{out} + R_{in})$ with R_{out} being the electrical resistance of the extracellular fluid and R_{in} the resistance inside the cytoplasm. Given the low resistivity of the extracellular medium, recordable extracellular signals are small, i.e., in the 5–100 μV range [8]. Recording electrodes have typical impedance at 1 kHz of a few tens of kohms to 1 MΩ, typically characterizes recording electrodes. In addition, compliant neural electrodes must provide reliable response when mechanically deformed.

3.2.1 Bending

Metallic electrodes embedded in flexible polyimide films can withstand prolonged bending in biological medium, both in vitro [24] and in vivo. Figure 4a illustrates the impedance modulus spectra of two polyimide micro-electrodes as a function of mechanical deformation. The electrodes are either held flat (unrolled) or rolled into a 1.5-mm outer diameter silicone tube. No changes are observed in the electrode response with bending, $Z \sim 1$ MΩ.

The impedance of the rolled electrodes was measured in six implanted animals at 3 months post-implantation (the implant design and functions are detailed in the next section). The exposed area of each electrode was 100 × 50μm^2, positioned halfway through the length of the implant. About 80% of the micro-channel electrodes (20 per implant) had relatively low impedances, which averaged about 1.2 ± 0.3 MΩ (at 1 kHz). The remaining electrodes were open circuited or had high impedances of >5 MΩ.

3.2.2 Stretching

Silicone electrodes can bend and stretch reversibly. Thin gold film on PDMS can sustain uni-axial stretch up to 100% strain without electrical failure and fatigue little when cycled by 20% strain thousands of times [12]. Mechanical deformation in vivo is often multidirectional. Therefore, the response of silicone electrodes to multi-axial strain must be evaluated. Figure 4b presents the electrical

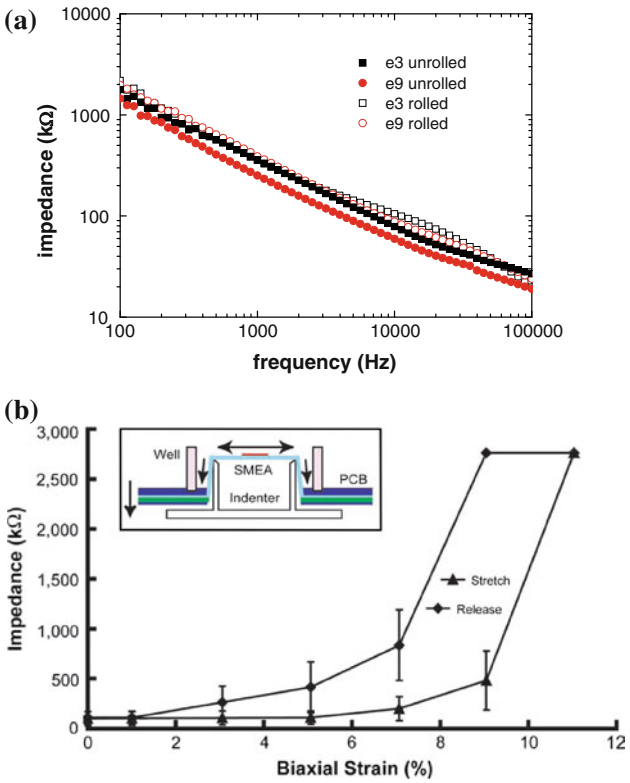

Fig. 4 Electrical impedance of compliant electrodes. **a** Impedance spectra of polyimide electrodes as a function of bending. The rolled electrodes are held under compression into a 1.5 mm inner diameter tube [24]. **b** Electrical impedance of a stretchable micro-electrodes as a function of applied radial strain. The electrode is cycled to 10% strain in 1 and 2% strain. *Inset*: sketch of the radial stretcher [11]

impedance of a stretchable micro-electrode prepared on PDMS (0.3 mm thick) and encapsulated with patternable silicone (15 μm thick) as a function of applied radial strain. Figure 4b inset shows a schematic of the experimental set-up: the silicone electrode array is placed against a hollow tube and pulled down against the tube inducing radial stretch in the elastomer. Before stretch, the electrode impedance at 1 kHz was 50–150 kΩ; it increased with applied radial strain and recovered during unloading to about its initial value. At biaxial strains of a few percentages, the impedance was found suitable for extracellular recording ($Z \sim 0.1$ MΩ–1 MΩ) [42].

The stretchability of the metallic electrodes relies on the built-in morphology of the gold film on PDMS. When a thin (<100 nm) evaporated gold film is deposited on PDMS substrate, the metal does not form as a continuous film but rather as a network of coalescent gold islands separated by micron scale cracks randomly dispersed throughout the film surface. Upon mechanical stretching, the gold ligaments, well adhered to the PDMS, tilt and deflect out-of-plane whilst the microcracks open and close [23]. This mechanism minimizes the mechanical stress and

related strain within the gold film, which can, therefore, expand up to twice its length without irreversible fracture.

Further, electrode impedance characterization as a function of maximum strain and strain rate, strain directions, cycling and extracellular fluid exposure is on-going to clarify the stretchability mechanisms, and to establish an accurate electrical model of stretchable micro-electrodes.

4 Discussion—example applications

We now proceed with the description of two novel neural interfaces using flexible or stretchable electrode arrays.

4.1 Bundle of micro-channel electrode arrays for peripheral nerve interface

Figure 5 presents a polyimide electrode implants designed for peripheral nerve repair. The neural interface is a 3D bundle of parallel micro-channels in an insulating PI substrate (Fig. 5a, b) hosting embedded micro-electrodes that are exposed to the interior of the channels (Fig. 3a). The outer dimensions of the polyimide implant are 4 mm in length and 1.5 mm diameter, matching the diameter of an adult rat's sciatic nerve. Each channel has a 100 × 100 μm cross-section. The implant is housed within a silicone tube, into the ends of which the proximal and distal stumps of the severed nerve are sutured. The micro-channel nerve interface is made initially as a flat plastic strip with open-topped channels and embedded micro-electrodes in polyimide using the processes described above. The strip is then rolled up into a cylinder so that the base layer of each turn of the roll roofs over the channels in the previous turn, yielding an array of closed micro-channels. The embedded electrodes (Fig. 3c) are connected by conductive tracks within the substrate to contact pads at the side of the device that can be linked to external electronic circuitry using a compliant cable. The polyimide contact pads are interfaced with electronic hardware using a commercial connector such as a zif connector. The recording sites are typically 100 × 50 μm^2 × 150 nm gold pads; 20 electrodes per implant are distributed in micro-channels in the third rolled layer where the bending radius is ∼600 μm [2]. Note that this third rolled layer was selected as it supports the most

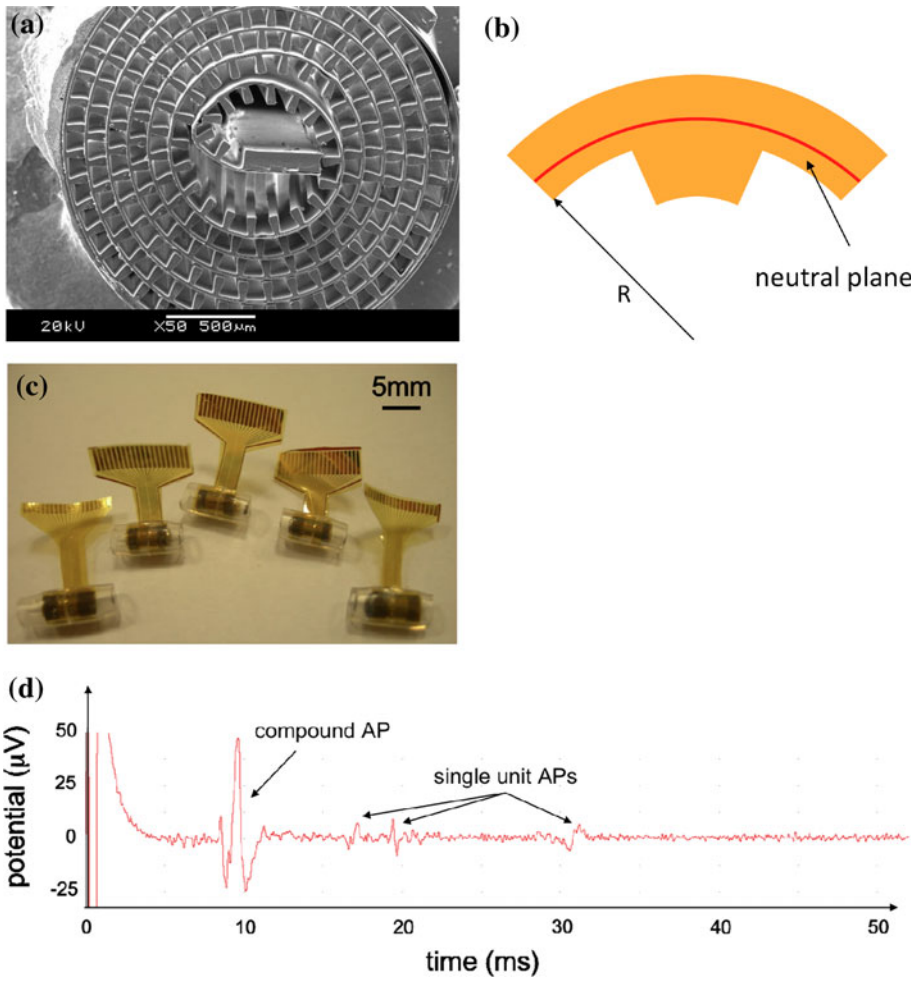

Fig. 5 Flexible micro-electrode arrays. **a** Cross-section of a rolled MEA obtained by scanning electron microscopy. The implant accommodates ∼190 micro-channels, of which 20 hosts one rolled micro-electrode (distributed in the third roll) [2]. **b** Macroscopic view of rolled MEAs inserted in silicone tube for implantation in rat's sciatic nerve. The tube has a 1.5 mm inner diameter. The compliant connector is sticking out of the roll for subcutaneous insertion. **c** Schematic cross-section of the channel pattern showing the structure neutral plane (strain ≈ 0%) at the electrode layer. **d** In vivo nerve activity recorded by a rolled micro-electrode at 12 weeks post-implantation. The recording site is positioned at the midpoint of the micro-channel, 2 mm away from each end. The sensory signals were generated by stimulating the rat's toe with needle electrodes (conduction distance approximately 70 mm) and averaging the potentials recorded by a single electrode (10 sweeps). A single stimulation pulse on the rat's toe excites several sensory fibres

robust axon outgrowth compared to channels located on the outer roll of the implant [21]. The metallic leads and electrodes are positioned at the mechanical neutral plane of the structure: the thickness of the polyimide substrate, encapsulation and channel along with the profile of the channels (Fig. 5b) were optimized to minimize the strain in the metal [21, 24].

The polyimide micro-channel electrode arrays support axon regeneration and vascularisation. Electron microscopy images taken from the distal nerve immediately after the implant illustrate regenerated "mini-nerves" along with blood vessel and regenerated myelinated axons. Robust vascularisation is observed through most micro-channels [21].

Action potentials can be reliably recorded extracellularly using the 3D polymeric implant. Figure 5d shows a typical extracellular recording in vivo obtained from one of the rolled micro-electrodes when stimulating the one toe with needle electrodes. The graph illustrates compound action potentials (typically >50 μV) and single fibre action potentials (typically >10 μV). More than half of the electrodes tested recorded waveforms, which demonstrates the robustness of our compliant electrode technology.

These first prototypes had 120 micro-channels each, 20 of which had a single electrode positioned at the midpoint of the channel. In theory, the micro-electrode layout could be designed to provide one electrode per channel throughout the cross-section of the device to maximize the number of efferent and afferent fibers that the interface could communicate with in the regenerated nerve. Furthermore, previous in vitro experiments indicate that a tripolar electrode configuration is recommended to minimize electrical noise and ensure that APs can be accurately discriminated [9]. More than 300 electrodes per implant is not realistic at this stage, mainly because of difficulties with lead-out from the device to external circuitry, but a few selected channels could host tripolar electrodes to enable optimal signal to noise performance.

The rolled micro-channel MEA sets the ground for promising bidirectional peripheral neuroprosthetics.

4.2 Stretchable micro-electrode arrays for in vitro brain trauma study

Traumatic brain injury (TBI) is caused by acceleration or blow to the head. As a result, brain tissues (often from the hippocampus involved in learning and memory) are suddenly deformed to strain levels inducing cell damage and ultimately death [43]. At the cellular level, normal neuronal electrophysiology is altered. In order to mimic such abrupt mechanical deformation and better assess its consequences on neuronal communication, we have designed an in vitro injury set-up allowing for simultaneous mechanical deformation of a hippocampal slice plated on a stretchable MEA, and field potentials monitoring before and immediately after injury. Figure 6a shows a top view of the experimental set up: the stretchable MEA is mounted between two PCBs (as shown Fig. 6a) fitted in the Multichannel Systems hardware, and sits above a cylindrical indenter (central ring Fig. 6a). The hippocampal slice is plated at the centre of the silicone MEA.

Figure 6b shows four graphs of field potentials recorded from a non-injured then injured slice. The top graphs illustrate stimulation-evoked activity from the hippocampal

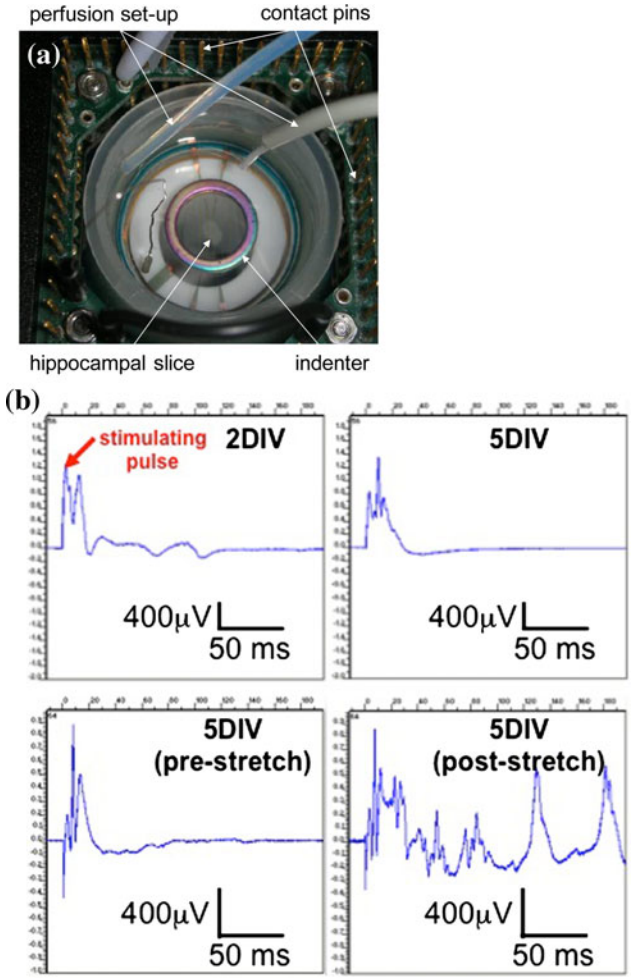

Fig. 6 Stretchable micro-electrode array. **a** Experimental set up. A hippocampal slice is seeded on a stretchable MEA and mounted over a hollow cylindrical indenter. Upon stretching, the stretchable membrane slides against the indenter and stretches the MEA and slice simultaneously. The SMEA is interfaced with a commercial MultiChannel Systems MEA60 recording system. **b** Typical field potentials recorded with the silicone MEA from a healthy (*top*) and mechanically injured, 8% radial strain, (*bottom*) slice. The slice was injured 5 days after plating (5DIV). Evoked activity was first recorded at 2DIV (*top left graph*). The four recordings were obtained from the very same electrode/slice interface [42]. Biphasic stimulating pulses are applied through two other electrodes of the array

slice recorded with one electrode of the stretchable MEA at two time points (2 and 5 days in vitro). Biphasic stimulating pulses are applied through two other electrodes of the array. The bottom graphs show the tissue response to sudden biaxial strain: before stretch, little activity is detected following onto the electrical stimulation. However, immediately after 8% strain biaxial stretch (within a few seconds of injury), both stimulated and spontaneous activities are recorded [42]. Note that the stretchable electrodes are not affected by the biaxial stretch, and do not impair the quality of the extracellular recordings. Such stretch signature could not be detected with conventional non-stretchable MEAs, which require the transfer and repositioning of the injured slice onto the array. Clearly stretchable MEAs provide a unique research platform to study TBI, and may possibly be implemented for in vivo neural interfaces.

5 Conclusion

Neural electrodes rely on an accurate and reliable interface between the neuronal cell(s) and the electrode recording sites. Advanced microtechnologies using polymers offer new opportunities for the development of active neural interfaces that go beyond the design of rigid and planar MEAs. We have optimized a set of fabrication processes for highly compliant interfaces without compromising on electrode performance, and demonstrated promising in vitro and in vivo extracellular recordings using flexible and stretchable micro-electrodes.

Acknowledgments This study was supported by the NINDS R21 0527794 and the NJ Commission on Science and Technology for BM, ZH, OG, the EPSRC-MRC Basic Technology Program (EP/C52330X) for SB, ET, IM, JF, SM, an MRC/Royal College of Surgeons of England fellowship for JF, and a University Research Fellowship of the Royal Society for SPL.

References

1. Adrega T, Lacour SP (2010) Stretchable conductors embedded in PDMS and patterned by photolithography: fabrication and electromechanical characterisation. J Micromech Microeng 20: 055025
2. Benmerah S et al (2009) Design and fabrication of neural implant with thick micro-channels based on flexible polymeric materials. Presented at the IEEE EMBS conference, Minneapolis
3. Cheng I-C, Wagner S (2009) Overview of flexible electronics technology. In: Wong WS, Salleo A (eds) Flexible electronics—materials and applications. Springer, New York, pp 1–28
4. Discher DE et al (2005) Cells feel and respond to the stiffness of their substrate. Science 310:1139–1143
5. Donaldson N et al (2008) Noise and selectivity of velocity-selective multi-electrode nerve cuffs. Med Biol Eng Comput 46: 1005–1018
6. Edell DJ (1986) A peripheral nerve information transducer for amputees: long-term multichannel recordings from rabbit peripheral nerves. IEEE Trans Biomed Eng 33:203–214
7. Fejtl M (2006) On micro-electrode array revival: its development, sophistication of recording, and stimulation. In: Taketani M, Baudry M et al (eds) Advances in network electrophysiology. Using multi-electrode arrays. Springer, Berlin, pp 24–37
8. FitzGerald J et al (2008) Microchannels as axonal amplifiers. IEEE Trans Biomed Eng 55:1136–1146
9. FitzGerald J et al (2009) Microchannel electrodes for recording and stimulation: in vitro evaluation. IEEE Trans Biomed Eng 56:1524–1534
10. Fontaine D et al (2010) Anatomical location of effective deep brain stimulation electrodes in chronic cluster headache. Brain 133:1214–1223
11. Graudejus O et al (2009) Characterization of an elastically stretchable microelectrode array and its application to neural field potential recordings. J Electrochem Soc 156:P85–P94
12. Graz I et al (2009) Extended cyclic uniaxial loading of stretchable gold thin-films on elastomeric substrates. Appl Phys Lett 94: 071902
13. Haftek J (1970) Stretch injury of peripheral nerve. J Bone Joint Surg 52B:354–365
14. Hai A et al (2009) Changing gears from chemical adhesion of cells to flat substrata toward engulfment of micro-protusions by active mechanisms. J Neural Eng 6:0066009
15. Hetke JF, Anderson DJ (2003) Silicon microelectrodes for extracellular recording. In: Finn WE, LoPresti PG (eds) Handbook of neuroprosthetic methods, chapter 7. CRC Press, Boca Raton
16. Hochberg L et al (2006) Neuronal ensemble control of prosthetic devices by a human with tetraplegia. Nature 442:164–171
17. http://professional.medtronic.com/devices/activa-pc/overview/index.htm, 2010
18. Janmey PA et al (2009) The hard life of soft cells. Cell Motil Cytoskelet 66:597–605
19. Kim S et al (2009) Integrated wireless neural interfaces based on the Utah electrode array. Biomed Microdevices 11:453–466
20. Krause M et al (2000) Extended gate electrode arrays for extracellular signal recordings. Sens Actuators B 70:101–107
21. Lacour SP (2009) Long micro-channel electrode arrays: a novel type of regenerative peripheral nerve interface. IEEE Trans Neural Syst Rehabil Eng (vol. online)
22. Lacour SP et al (2005) Stretchable micro-electrode arrays for dynamic neuronal recording of in vitro mechanically injured brain. In: Proceedings of the fourth IEEE conference on sensors, pp 617–620
23. Lacour SP et al (2006) Mechanisms of reversible stretchability of thin metal films on elastomeric substrates. Appl Phys Lett 88: 204103-1–204103-3
24. Lacour SP et al (2008) Polyimide micro-channel arrays for peripheral nerve regenerative implants. Sens Actuators A 147: 456–463
25. Maghribi M et al (2002) Stretchable micro-electrode array. In: Second annual international IEEE-EMBS special topic conference on microtechnologies in medicine and biology, pp 80–83
26. Meacham KW et al (2008) A lithographically-patterned, elastic multi-electrode array for surface stimulation of the spinal cord. Biomed Microdevices 10:259–269
27. Morrison B et al (1998) In vitro central nervous system models of mechanically induced trauma: a review. J Neurotrauma 15:911–928
28. Morrison B et al (2006) An in vitro model of traumatic brain injury utilising two-dimensional stretch of organotypic hippocampal slice cultures. J Neurosci Methods 150:192–201
29. Moshayedi P et al (2010) Mechanosensitivity of astrocytes on optimized polyacrylamide gels analyzed by quantitative morphometry. J Phys Condens Matter 22:194114

30. MultiChannelSystems (2010, 21/05/2010) Microelectrode arrays
31. Navarro X et al (2005) A critical review of interfaces with the peripheral nervous system for the control of neuroprostheses and hybrid bionic systems. J Peripher Nerv Syst 10:229–258
32. Périchon-Lacour S et al (2003) Stretchable gold conductors on elastomeric substrates. Appl Phys Lett 82:2404–2406
33. Polasek H et al (2009) Intraoperative evaluation of the spiral nerve cuff electrode on the femoral nerve trunk. J Neural Eng 6:066005
34. Polikov VS et al (2005) Response of brain tissue to chronically implanted neural electrodes. J Neurosci Methods 148:1–18
35. Rehfeldt F et al (2007) Cell responses to the mechanochemical microenvironment—implications for regenerative medicine and drug delivery. Adv Drug Deliv Rev 59:1329–1339
36. Rutten WLC et al (1995) 3D neuroelectronic interface devices for neuromuscular control: design studies and realisation steps. Biosens Bioelectr 10:141–153
37. Suo Z et al (1999) Mechanics of rollable and foldable film-on-foil electronics. Appl Phys Lett 74:1177–1179
38. Wagner S et al (2005) Chapter 14: mechanics of TFT technology on flexible substrates. In: Crawford GP (ed) Flexible flat panel displays. Wiley, Chichester, pp 263–283
39. Williams JC et al (2007) Complex impedance spectroscopy for monitoring tissue responses to inserted neural implants. J Neural Eng 4:410–423
40. Wilson BS, Dorman MF (2008) Cochlear implants: a remarkable past and a brilliant future. Hear Res 242:3–21
41. Yoshida K, Riso R (2004) Peripheral nerve recording electrodes and techniques. In: Horch KW, Dhillon GS (eds) Neuroprosthetics. Theory and practice. World Scientific Publishing Co., New Jersey, pp 683–744
42. Yu Z et al (2009) Monitoring hippocampus electrical activity in vitro on an elastically deformable microelectrode array. J Neurotrauma 26:1135–1145
43. Zhang L et al (2001) Biomechanics of brain trauma. Neurol Res 23:144–156